

An assessment of structural enthalpy and crystallization pathways of $\text{Mg}_{65}\text{Zn}_{30}\text{Ca}_5$ bulk metallic glass and amorphous films

Scott Gleason, David Miskovic, Nicholas Hamilton, Kevin Laws, Michael Ferry

UNSW Australia
School of Material Science and Engineering

July 28, 2017

ABSTRACT

The structural nature and thermal stability of amorphous alloys is highly dependent on the method by which they are produced, i.e. their relaxation rate upon cooling. Both bulk samples and metallic glass films of $\text{Mg}_{65}\text{Zn}_{30}\text{Ca}_5$ were produced by copper mold casting and direct current (DC) magnetron sputtering onto aluminium substrates, respectively. Comparisons between structural enthalpy, crystallization pathways, relaxation and crystallization kinetics of the bulk samples and films were examined by elevated temperature XRD and DSC. Compared with equivalent experiments on the bulk alloy, results for the thin films show distinct differences in structural enthalpy and deviations from the expected crystalline phase evolution, displaying minor peak shifts, failure of some phases to evolve, and variations in the evolution rates.

TABLE OF CONTENTS

ABSTRACT	i
TABLE OF CONTENTS	1
1 INTRODUCTION	1
2 METHOD	1
2.1 Master alloy	1
2.2 DC magnetron sputtering	1
2.3 Stylus Profiler	2
2.4 DSC characterization	2
2.5 XRD characterization	2
3 RESULTS	2
4 DISCUSSION	3
5 CONCLUSIONS	4
6 ACKNOWLEDGEMENTS	4
7 REFERENCES	4

1 INTRODUCTION

The structural nature and thermal stability of amorphous alloys is highly dependent on the method by which they are produced, i.e. their relaxation rate upon cooling. Both bulk samples and metallic glass films of $\text{Mg}_{65}\text{Zn}_{30}\text{Ca}_5$ were produced by copper mold casting and direct current (DC) magnetron sputtering onto aluminium substrates, respectively. Comparisons between structural enthalpy, crystallization pathways, relaxation and crystallization kinetics of the bulk samples and films were examined by elevated temperature XRD and DSC. Compared with equivalent experiments on the bulk alloy, results for the thin films show distinct differences in structural enthalpy and deviations from the expected crystalline phase evolution, displaying minor peak shifts, failure of some phases to evolve, and variations in the evolution rates.

Key sources ^{Zhang Zhang Zhang 2012} [1, 2] [3]

2 METHOD

2.1 Master alloy

The master alloy of $\text{Mg}_{65}\text{Zn}_{30}\text{Ca}_5$ was produced using high-purity elements of Mg (99.85 wt%), Zn (99.995 wt%), and Ca (99.8 wt%). The alloy was prepared by induction melting in boron nitride coated graphite crucibles, purged with Ar (99.997 vol.% purity) five times, and protected with a circulating Ar atmosphere. Alloy homogeneity was ensured by heating and cooling through a cycle of 700°C, 385°C, 650°C, 385°C, 650°C to a casting temperature of 500 °C and 450°C for for injection and gravity casting respectively. Bulk amorphous $\text{Mg}_{65}\text{Zn}_{30}\text{Ca}_5$ rod of 2.5mm diameter and plates of thickness of $XX\mu\text{m}$ were produced by copper mold injection casting. The 25.4mm diameter targets were prepared from a cylindrical copper mold gravity castings sectioned to thicknesses of 3.25mm. All samples and targets were stored under Ar when not being examined or used.

2.2 DC magnetron sputtering

Films were produced from an in-house DC magnetron sputtering facility with Ar working gas (99.997 vol.% purity). The power was 15W, typical voltage of 290 – 350V, nominal chamber pressure of 1 bar, substrate temperature of 25 °C, and Ar flow of 3.01 SCCM. Films were deposited directly onto to Al DSC lid substrates. Depositions were for a period of 35 minutes. Deposition rate was estimated at 1.2nm/s.

2.3 Stylus Profiler

Nominal film thickness was measured by a stylus profiler (Dektak 2A, Bruker, Germany). A glass slide was placed under the substrates within the sputtering chamber, allowing the substrates to act as a mask. Profile measurements were taken by measuring the height difference between the bare glass and the film covered glass. This film thickness was used to estimate the sputter deposition rate.

2.4 DSC characterization

Isochronic DSC (204 F1 Phoenix, Netzsch, Selb, Germany) was carried out in Al crucibles under a protective Ar (99.997 vol.% purity) atmosphere. Scans were performed at heating rates of 5 to 100K/min.

For annealed XRD the samples were heat treated in the DSC by heating to the desired temperature at 20K/min followed by Ar quenching to room temperature.

2.5 XRD characterization

Annealing XRD (PANalytical, Empyrean, Cu K_α X-ray source, $\lambda = 1.541\text{\AA}$) was performed at room temperature. (Generator Voltage 45, Tube Current 40, Scan Step Size 0.0262606, Time per Step 397.29).

Dynamic XRD (Bruker, D8, Cu K_α X-ray source, $\lambda = 1.541\text{\AA}$) was performed by raising temperature at a rate of 20K/min and performing scans *in situ*. The first scan was performed at 35 °C, then 75 °C, after which temperature was raised in 5K increments. The 2θ scans from 31 – 60° were completed within 1092sec (18min, 12sec) to minimise the effects of recrystallisation during the experiment. (Generator Voltage 45, Tube Current 100, Scan Step Size 0.02, Time per Step 134.4).

3 RESULTS

During the 35 minute depositions an average temperature rise of 3 – 4 °C was observed. Nominal film thickness was about 2.5 μm giving a deposition rate of 1.2nm/s.

Relaxed differential scanning calorimetry (DSC) of bulk material taken at different heating rates was used to establish the fragility of the $\text{Mg}_{65}\text{Zn}_{30}\text{Ca}_5$ system. From the equations

... a fit of $\beta^{-1} = 1.338E - 16e^{5274(\frac{1}{T-T_0})}$ with Adj. $R^2 = 0.972$ was established. This give a $D^* = 20.4$ which using $D^* = 590/(m - 16)$ Shuai2014 [4, 5] gives a fragility $m = 44.9$.

Heating Rate β K/min	T_g	T_{x1}	T_{x2}	T_{x3}	T_{x4}	T_{x5}
100	136.1	152.4	193.4	201.8	240.2	262.4
80	132.0	151.6	194.4	201.9	238.2	260.3
60	129.6	151.6	190.0	197.8	232.9	259.0
40	126.6	151.0	189.0	200.0	226.4	254.7
30	126.2	147.4	187.0	198.4	221.0	251.1
20	125.1	147.3	188.4	197.0	216.0	246.8
15	123.8	146.0	186.2	195.6	212.2	243.9
10	123.5	142.3	183.4	192.9	207.4	239.8
5	120.5	139.2	179.7	187.5	199.8	232.7

Table 1: Bulk $Mg_{65}Zn_{30}Ca_5$ alloy onset temperatures for the various DSC heating rates β . All temperatures are in $^{\circ}C$.

Heating Rate β K/min	T_g	T_{x1}	T_{x2}	T_{x3}	T_{x4}	T_{x5}
100	108.5	135.1	0.0	177.3	0.0	240.3
80	106.0	128.2	0.0	165.6	0.0	238.8
60	107.3	129.1	0.0	176.1	0.0	237.8
40	100.2	117.6	0.0	170.7	0.0	234.2
30	95.3	114.4	0.0	169.5	0.0	232.5
20	95.5	110.0	0.0	170.5	0.0	229.4
15	92.5	107.4	0.0	168.8	0.0	224.0

Table 2: Film $Mg_{65}Zn_{30}Ca_5$ alloy onset temperatures for the various DSC heating rates β . All temperatures are in $^{\circ}C$.

4 DISCUSSION

The use of a 60K DSC heating rate compared to the more commonly used 20K rate [sources] shifts peaks for the bulk $Mg_{65}Zn_{30}Ca_5$ alloy about 8 - 15 degrees higher. This higher heating rates were used because crystallization events for the films were different to differentiation at the lower heating rate. Films show little shift to high temperature peaks with increases heating rates, but large shifts with relaxation. Bulk show the opposite behaviour, larger peaks shifts with higher heating rates and little shift with relaxation.

5 CONCLUSIONS

6 ACKNOWLEDGEMENTS

Yu Wang for his assistance with XRD experimentation and Rietveld refinement.

7 REFERENCES

- hang2013 [1] Y. N. Zhang, G. J. Rocher, B. Briccoli, D. Kevorkov, X. B. Liu, Z. Altounian, and M. Medraj. Crystallization characteristics of the Mg-rich metallic glasses in the Ca-Mg-Zn system. *Journal of Alloys and Compounds*, 552:88–97, 2013.
- hang2012 [2] Yi-Nan Zhang, Dmytro Kevorkov, Xue Dong Liu, Florent Bridier, Patrice Chartrand, and Mamoun Medraj. Homogeneity range and crystal structure of the $\text{Ca}_2\text{Mg}_5\text{Zn}_{13}$ compound. *Journal of Alloys and Compounds*, 523:75–82, 2012.
- hang2011 [3] Yi-Nan Zhang, Dmytro Kevorkov, Florent Bridier, and Mamoun Medraj. Experimental study of the Ca-Mg-Zn system using diffusion couples and key alloys. *Science and Technology of Advanced Materials*, 12(2):025003, 2011.
- Cao2013 [4] Jake Diablo Cao. Processing and properties of biocompatible metallic glasses, 2013.
- Cao2012 [5] J D Cao, K J Laws, N Birbilis, and M Ferry. Potentiodynamic polarisation study of bulk metallic glasses based on the Mg-Zn-Ca ternary system. *Corrosion Engineering, Science and Technology*, 47(5):329–334, 2012.
- Gu2005 [6] X. Gu, G.J. Shiflet, F.Q. Guo, and S.J. Poon. Mg-Ca-Zn bulk metallic glasses with high strength and significant ductility. *Journal of Materials Research*, 20(08):1935–1938, 2005.
- Zhou2013 [7] X. Zhou, K. D. Ralston, K. J. Laws, J. D. Cao, R. K. Gupta, M. Ferry, and N. Birbilis. Effect of the degree of crystallinity on the electrochemical behavior of $\text{Mg}_{65}\text{Cu}_{25}\text{Y}_{10}$ and $\text{Mg}_{70}\text{Zn}_{25}\text{Ca}_5$ bulk metallic glasses. *Corrosion*, 69(8):781–792, 2013.
- Wang2013 [8] Jingfeng Wang, Song Huang, Yang Li, Yiyun Wei, Xingfeng Xi, and Kaiyong Cai. Microstructure, mechanical and bio-corrosion properties of Mn-doped Mg-Zn-Ca bulk metallic glass composites. *Materials Science and Engineering: C*, 33(7):3832–3838, 2013.

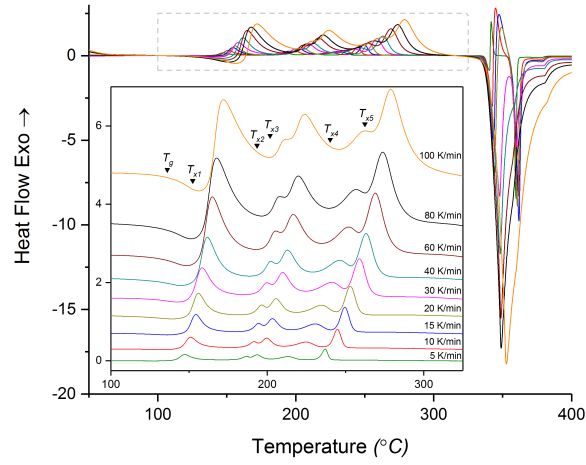


Figure 1: Bulk $\text{Mg}_{65}\text{Zn}_{30}\text{Ca}_5$ relaxed at 120°C for 10 minutes and heated at various heating rates. The insert stacks the DSC curves and labels the T_g and T_x es of the $100\text{K}/\text{min}$ sample.

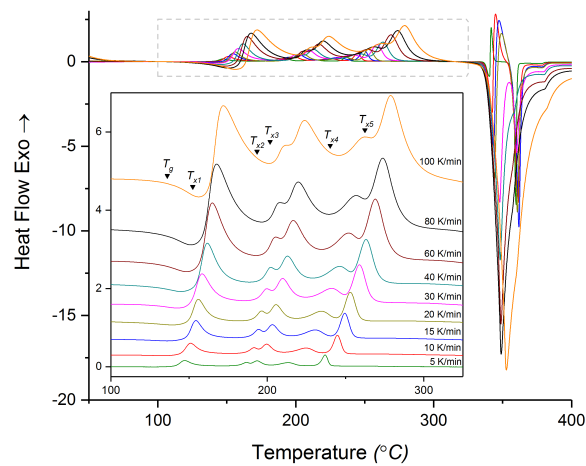


Figure 2: Unrelaxed film $\text{Mg}_{65}\text{Zn}_{30}\text{Ca}_5$ heated at various heating rates. The insert stacks the DSC curves and labels the T_g and T_x es of the $100\text{K}/\text{min}$ sample.

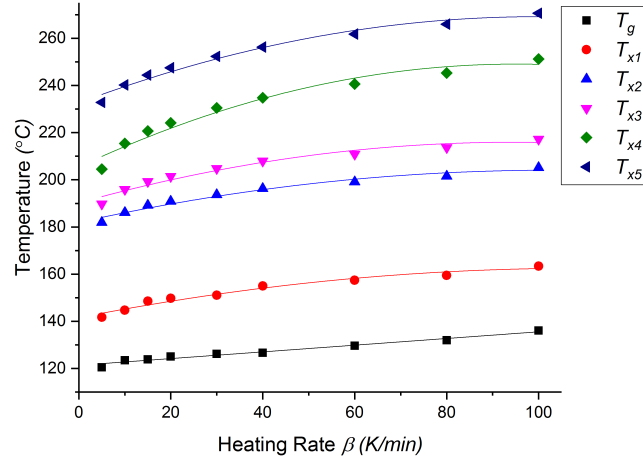


Figure 3: The T_g s and T_x es of the bulk $\text{Mg}_{65}\text{Zn}_{30}\text{Ca}_5$ at all heating rates.

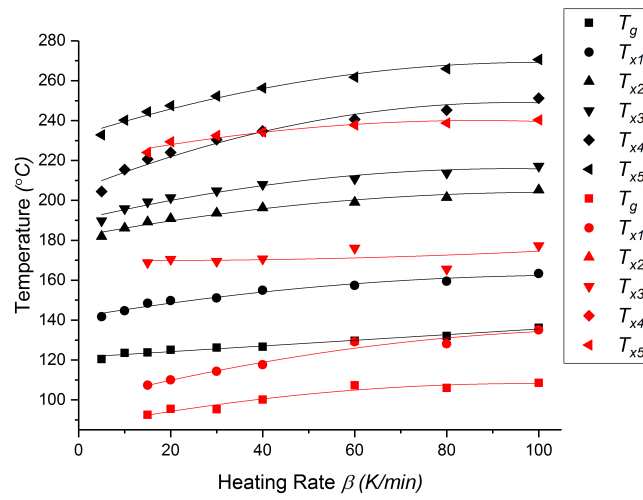


Figure 4: The T_g s and T_x es of the bulk and film $\text{Mg}_{65}\text{Zn}_{30}\text{Ca}_5$ at all heating rates.

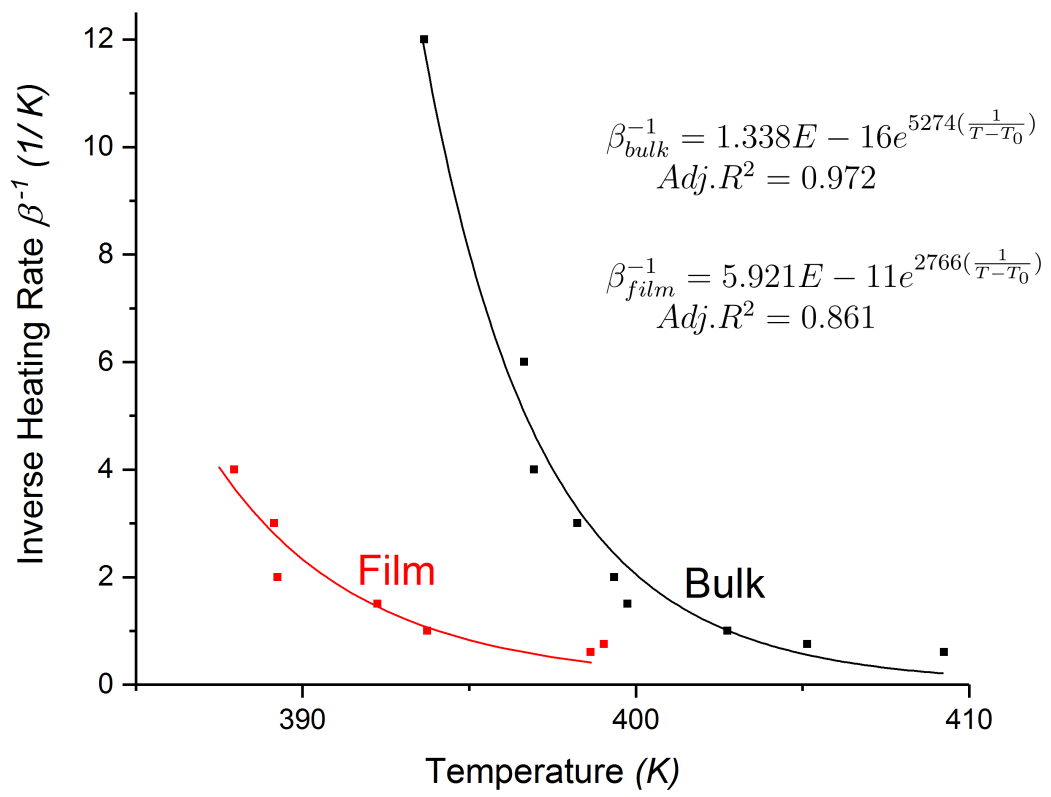


Figure 5: Fitted fragility for the $Mg_{65}Zn_{30}Ca_5$ system obtained by DSC at various heating rates

m_mValue

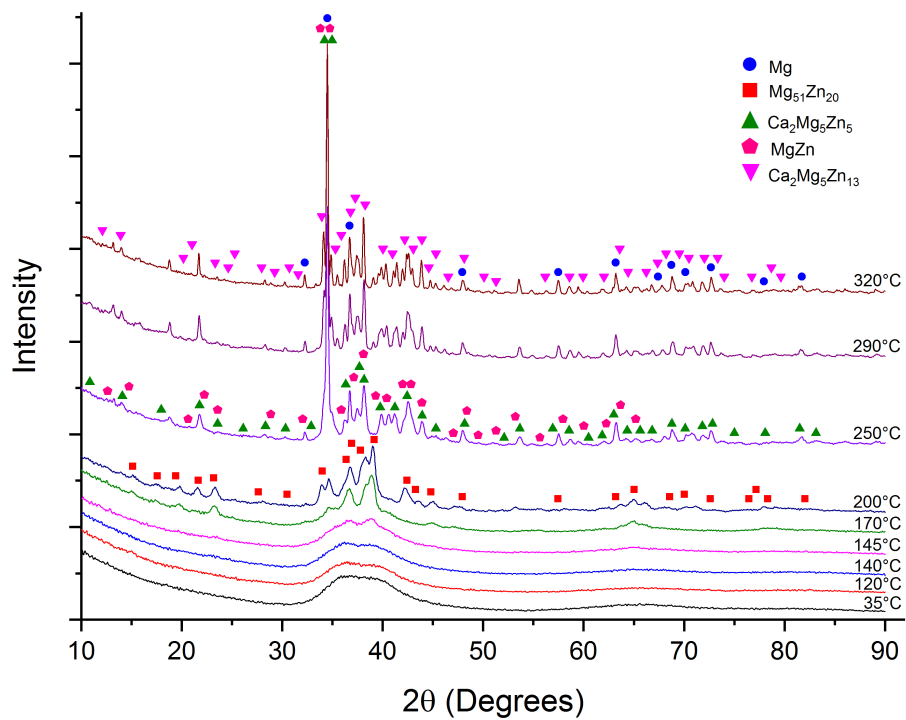


Figure 6: XRD pattern for Bulk $\text{Mg}_{65}\text{Zn}_{30}\text{Ca}_5$ heated through several crystallization peaks identified from DSC

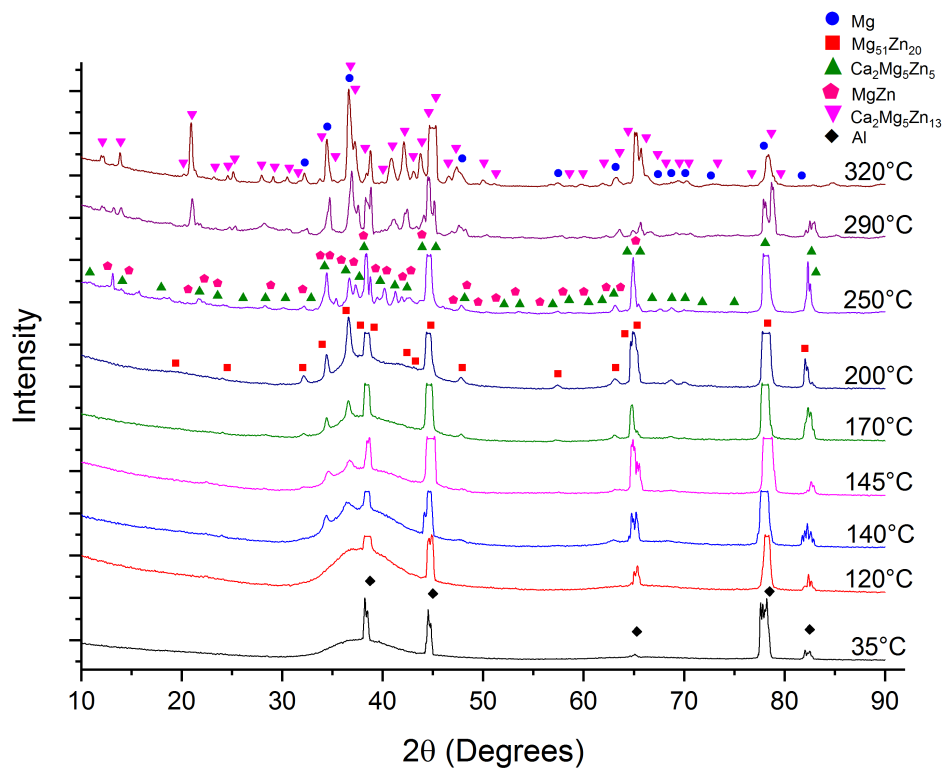
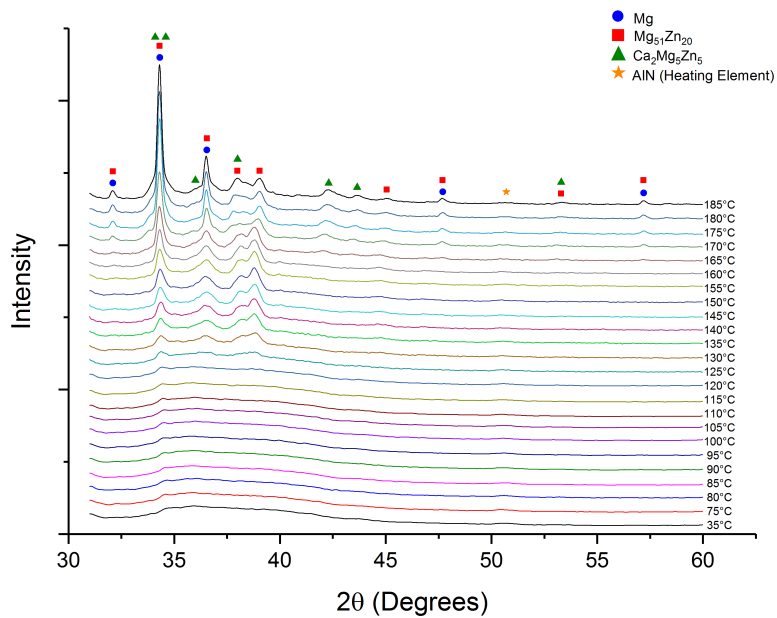
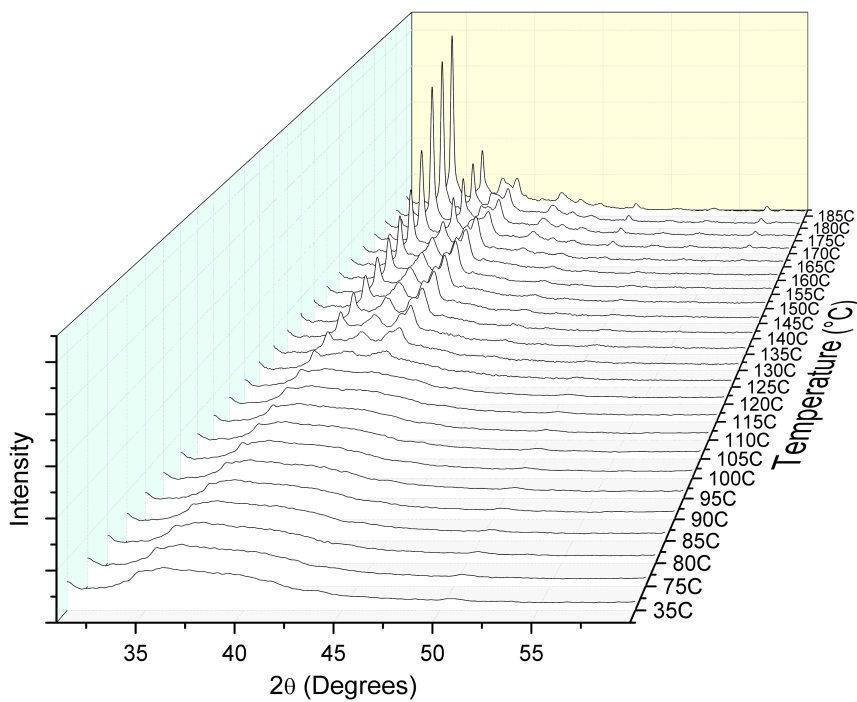


Figure 7: XRD pattern for Film $\text{Mg}_{65}\text{Zn}_{30}\text{Ca}_5$ heated through several crystallization peaks identified from DSC

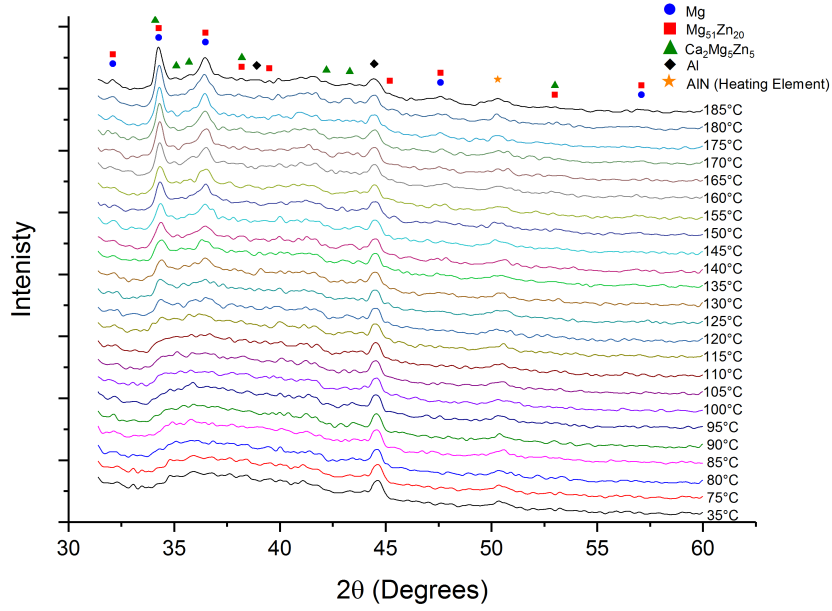


(a)

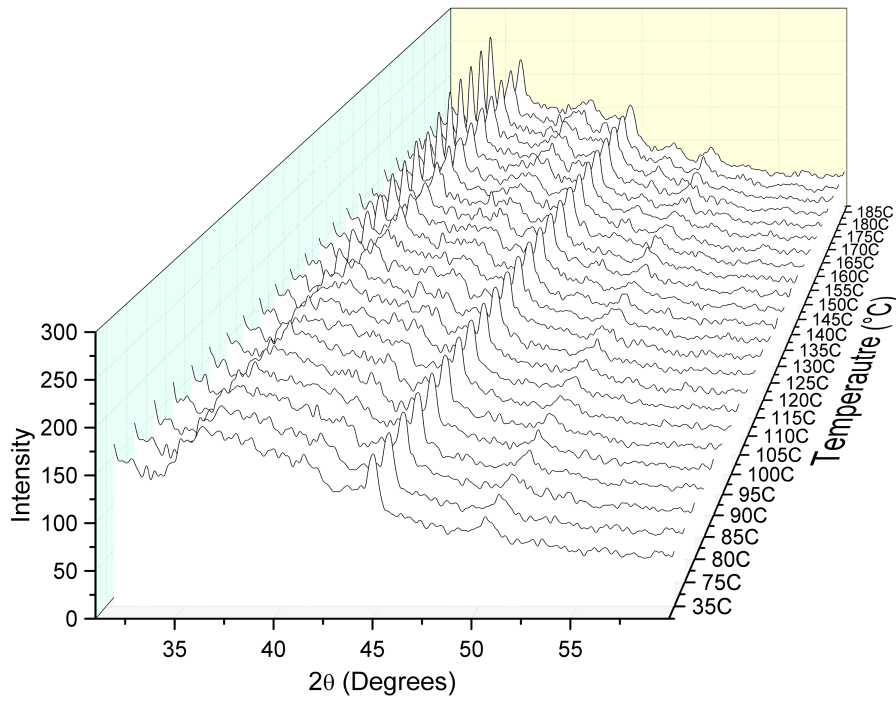


(b)

Figure 8: (a) Stacked X-ray diffraction (XRD) patterns from the incremental heating of bulk $\text{Mg}_{65}\text{Zn}_{30}\text{Ca}_5$. (b) Cascading XRD patterns from the incremental heating of bulk $\text{Mg}_{65}\text{Zn}_{30}\text{Ca}_5$.



(a)



(b)

Figure 9: (a) Stacked XRD patterns from the incremental heating of film $\text{Mg}_{65}\text{Zn}_{30}\text{Ca}_5$. (b) Cascading XRD patterns from the incremental heating of film $\text{Mg}_{65}\text{Zn}_{30}\text{Ca}_5$.